MADRID
inter.noise 2019
June 16 - 19
NOISE CONTROL FOR A BETTER ENVIRONMENT

Transmission paths and their influence on power transformers noise

Linhares, Cassiano[1]; Coutinho, Cristiano P.; Teixeira, Ricardo; Santo, João E.; Tavares, Sérgio M.O.; Novais, Catherine; Pinto, Marta; Mendes, Hélder

Efacec
Porto, Portugal

Palacios, Juan Pedro; de Gregorio, Alfredo

ESI Group Hispania
Madrid, Spain

ABSTRACT

The accelerated growth on electrical energy consumption has led to an increased number of substations near urban areas and their rated power. As a result, transformers radiated noise has become a problem to utilities, requiring manufacturers to invest in the development of quieter equipment. The vibration and noise generated within the active part of the power transformers is transmitted through either fluid-structure or structural-structural interactions. Therefore, the oil is responsible for a part of the vibration transmission in a power transformer; the other part is transmitted through structural connections between components, such as the active part and tank. In the present research the transmission paths of vibration and noise are quantified and their influence on the transformer radiated noise is discussed. With these objectives, a multiphysics numerical model was developed consisting in three sequential simulations.

The first stage is an electromagnetic magnetic analysis of the active part, to obtain the typical loading conditions of a power transformer. Then, through a modal analysis the vibration behavior of the structure is extracted in in the format of a modal base. At last, the internal/external vibro-acoustic problem is solved through the Finite Element And Boundary Element Methods, and the irradiated acoustic power is predicted.

Keywords: Power Transformer, Transmission Paths, Noise Level, FEM/BEM Model
I-INCE Classification of Subject Number: 76

[1]cassiano.linhares@efacec.com

1. INTRODUCTION

Noise pollution, or the exposure to unwanted sounds, can harm the balance of an ecosystem affecting both human and the general wellbeing and health. With technological development and the population growth, cities are becoming more crowded, larger and, consequently, noisier. The noise pollution is then becoming an issue of increasing concern [1]. A typical example of this are the biggest metropolitan areas of the world such as New York and Tokyo; their power supply systems are associated with relatively low sound level in urban areas, however, one of the main components of any power supply system, a power transformer, can become an annoyance. Back in the day, these used to be located far from urban areas, where the noise was not a concern; however with the exponential growth of the cities this is no longer possible, and bigger and bigger transformers need to be in the vicinity of populated areas enhancing the need to low noise solutions.

1.1.1. Description of noise sources

In a power transformer, the noise is mainly generated by the periodic mechanical deformation of both core and windings, under the influence of fluctuating electromagnetic flux associated with the alternated current supplied [2, 3] and Lorentz forces for the latter [4]. The magnetostrictive properties of the core material - electric steel - induce vibration due to the magnetostrictive strain, whose harmonics are twice those of the magnetic flux. Other noise sources are related with the reluctance Lorentz forces. The former are due to residual air-gaps between core laminations, while the latter occur in the windings due to the interaction between current and magnetic field [5]. Cooling systems also contribute to the radiated noise level, generating sound with a broader frequency range [2].

1.1.2. Transmission paths

In an oil immersed power transformer, the vibration generated in the core can be transmitted to the tank via two groups of path. One of them are the structural paths, created by mechanical joints between the active part and the tank. The other group are the acoustic paths, typically created by the insulation oil, via structure-to-fluid and fluid-to-structure coupling. Due to its complexity the latter group is not often adressed, although it is known that the insulation oil has a significant effect on both the dynamic and acoustic behaviors of a power transformer [6, 7].

1.1.3. Vibro-acoustics simulation

A vibro-acoustic problem, depending on its caracteristics, can be classified as internal, external or mixed internal/external problems. In the area of power transformers, the analysis of transmission and irradiation of noise can be classified as a mixed problem; in this class of problems, the structure is in contact with several acoustic domains, with one of them being unbounded. Previous researches are usually based on the use commercial simulation softwares, often with a combination of the Finite Element Method (FEM) and the Boundary Element Method (BEM) [8, 9].

2.2.1. Electromagnetic forces

Through an electromagnetic analysis, the magnetic flux density in the core of a power transformer can be predicted. If the material nonlinearity (due to the magnetic behavior of the electrical steel) is to be considered, then a transient analysis has to be performed. In this case, the three-dimensional electromagnetic transient problem to be solved is described by the following relevant set of equations:

$$\mathbf{B} = \mu \mathbf{H} \tag{1}$$

$$\mathbf{J} = \sigma \mathbf{E} \tag{2}$$

$$\nabla \times \mathbf{E} = -\frac{\partial \mathbf{B}}{\partial t} \tag{3}$$

$$\nabla \cdot \mathbf{B} = 0 \tag{4}$$

$$\nabla \times \frac{1}{\sigma} \nabla \times \mathbf{H} + \frac{\partial \mathbf{B}}{\partial t} = 0 \tag{5}$$

Where $\mathbf{E}$ is the electric field density, $\mathbf{B}$ is the magnetic flux density, $\mathbf{H}$ is the magnetic field strength, $\mathbf{J}$ is the current density, μ is the magnetic permeability and σ is the electric condutivity.

Power transformers under no-load conditions are subjected to reluctance (surface) - $\mathbf{f}_A^R$ - and magnetostriction (volume) - $\mathbf{f}_V^{MS}$ - force densities, generated on the magnetic circuit; in addition to those, under load conditions, there are Lorentz (volume) - $\mathbf{f}_V^L$ - force densities exciting the transformer windings. Through post-processing of the magnetic flux density, those force surface and volume densities can be calculated as follows, [10, 11]:

$$\bar{\mathbf{S}} = \frac{1}{\mu} \begin{bmatrix} \mathbf{B}_x^2 - \mathbf{B}^2/2 & \mathbf{B}_x\mathbf{B}_y & \mathbf{B}_x\mathbf{B}_z \\ \mathbf{B}_x\mathbf{B}_y & \mathbf{B}_y^2 - \mathbf{B}^2/2 & \mathbf{B}_y\mathbf{B}_z \\ \mathbf{B}_x\mathbf{B}_z & \mathbf{B}_y\mathbf{B}_z & \mathbf{B}_x^2 - \mathbf{B}^2/2 \end{bmatrix} \tag{6}$$

$$\mathbf{F} = \frac{1}{\mu_0} \int_A \mathrm{dA} \bar{\mathbf{S}} \cdot \mathbf{n} \tag{7}$$

$$\mathbf{f}_A^R = \frac{\mathbf{F}}{A_s} \tag{8}$$

$$\mathbf{f}_V^{MS} = \frac{1}{V_e} \sum_{i=1}^{N} \mathbf{F_i} \tag{9}$$

$$\mathbf{f}_V^L = \frac{1}{V} \int_V (\mathbf{J} \times \mathbf{B}_L) \mathrm{dV} \tag{10}$$

Where $\bar{\mathbf{S}}$ is the Maxwell stress tensor, $\mathbf{B}$, $\mathbf{B}_x$, $\mathbf{B}_y$, $\mathbf{B}_z$ are the magnetic flux density and the respective components at the center of the surface face (respectively in the x, y and z orthogonal directions), μ is the permeability of the near element, μ_0 is the vacuum or air space permeability, $\mathbf{n}$ is outward normal direction of the face, A_s is the surface area, V_e

is the volume of an element, N is the number of surfaces of the element, $\mathbf{J}$ is the current density in a element, and $\mathbf{B}_L$ is the leakage flux density between primary and secondary windings.

2.2.2. Numerical approaches to vibro-acoustics simulation

To cover the entire frequency range of interest, the analysis must take into account the large number of acoustic and structural modes contributing to the dynamic response. Modal analysis procedures can be extended to predict the interior acoustic environment by identifying the structural modes of the surfaces and acoustical modes of the interior space. Comercial softwares, and in particular ESI VA-One, provide many options for predicting vibro-acoustic response.

For low frequency range, two different deterministic methods exist to deal with the acoustic phenomena. The first one is the Finite Element Method (FEM) consisting in introducing infinite elements to deal with exterior diffuse field (unbounded domain) and meshing the air space around and the acoustic domain inside the structure. Nevertheless, the FEM approach leads to direct sparse matrix linear system to be solved which is a very interesting point. The second one is the Boundary Element Method (BEM) which consists in meshing only the surfaces of the fluid domain and is very suitable to handle free edges, both interior/exterior spaces. For low frequency range, the industry standard for performing vibro-acoustic analyses consists of fully coupling a Finite Element Model (FEM) of the structure with a Boundary Element Model (BEM) of the fluid [12]. This is the one implemented in the present case study.

2.2.1 Finite Element Method

The Finite Element Method (FEM) is the most widely used structural modelling technique in structural analysis. The structural domain equations of motion are expressed in terms of the nodal displacements, while in the acoustic domain, the pressure field is the unknown. The matrix governing equation for the Finite Element Structure is given by:

$$M\ddot{u}_s + Ku_s = F_s \tag{11}$$

Where, u_s is the nodal displacement vector, M and K are the mass and stiffness matrix and F_s are the external forces applied to the structure. VA One uses a modal approach to solve these equation, converting the equation to:

$$M_q\ddot{q}_s + K_q q_s = F_q \tag{12}$$

Where, M_q and K_q are the modal Mass and Stiffness matrix, F_q, the modal external forces and q_s the generalized coordinates of the system. Damping is latter set as a loss factor in terms of modal damping.

Additionally, for the acoustic domain, the governing equations for the acoustic fluid are given by the equations of motion, the continuity equation and the constitutive equation, written respectively as:

$$\rho_0 \frac{\partial^2 u_F}{\partial t^2} + \nabla p_F(t) = 0 \tag{13}$$

$$\frac{\partial \rho_F(t)}{\partial t} + \rho_0 \nabla \frac{\partial u_F(t)}{\partial t} = q_F(t) \tag{14}$$

$$p_F(t) = c_0^2 \rho_F(t) \tag{15}$$

In these equations, $u_F(t)$ is the displacement of the fluid particles, $p_F(t)$ is the dynamic pressure, $\rho_F(t)$ is the dynamic density and $q_F(t)$ is the added fluid mass per unit volume. These equation can be discretized and perform a modal approach, resulting in a matrix equation in the following way:

$$M_F \ddot{p} + K_F p = F_p \tag{16}$$

Where: M_F is the fluid equivalent mass matrix, K_F is the fluid equivalent stiffness matrix, F_p is the term for external input forces

At the boundary between the structural and fluid domains, the fluid particles and the structure moves together in the normal direction of the boundary. Considering this continuity and the relation between pressure and acceleration in the fluid particles:

$$\nabla p_F = -\rho_0 \frac{\partial^2 u_F(t)}{\partial t^2} \tag{17}$$

then, the boundary forces for the acoustic domain can be expressed in terms of structural acceleration. This is the basis to obtain a coupling matrix C_{SF} between the pressure in the fluid nodes and the displacements of the structural nodes. Then, the matrix equations for the structure (Equation 12) and for the fluid (Equation 16) can be merged in the following unsymmetric equation:

$$\begin{pmatrix} M_s & 0 \\ \rho_0 c_0^2 C_{SF}^T & M_F \end{pmatrix} \begin{Bmatrix} \ddot{q}_s \\ \ddot{p} \end{Bmatrix} + \begin{pmatrix} K_s & C_{SF} \\ 0 & K_F \end{pmatrix} \begin{Bmatrix} q_s \\ p \end{Bmatrix} = \begin{Bmatrix} F_s \\ F_p \end{Bmatrix} \tag{18}$$

2.2.2 Boundary Element Method for Acoustic Domains

Concerning the fluid, we consider the propagation of time harmonic acoustic waves in a homogeneous isotropic acoustic medium (which can be either finite or infinite) as described by the well-known Helmholtz equation:

$$\nabla^2 p(x) + k^2 p(x) = 0 \tag{19}$$

Where, p is the pressure field and k the wave number. The coupling is defined considering the continuity of normal displacements (Newmann boundary condition):

$$\frac{\partial p}{\partial n} = \rho_f \omega^2 u \tag{20}$$

In the BEM formulation the Helmholtz equation is converted into a boundary integral equation, making use of the weight function:

$$G(x, y) = \frac{e^{-ikr}}{4\pi r}; \tag{21}$$

Were, $r = |x - y|$. Then, from it, the integral Green function is obtained:

$$C(x)p(x) + \int_{\Gamma_f} p(y) \frac{\partial G(x, y)}{\partial n} \mathrm{d}\Gamma = \int_{\Gamma_\mathrm{f}} \mathrm{G(x, y)} \frac{\partial \mathrm{p(y)}}{\partial \mathrm{n}} \mathrm{d}\Gamma \tag{22}$$

Where, $C(x)$ is a coefficient dependent of the position of point x. For infinite domains, another boundary condition is taken in terms of the Sommerfield radiation. The Equation 22 can be then discretized and converted to matricial form.

3. VIBRO-ACOUSTIC MODEL OF A POWER TRANSFORMER

This case study adressed the vibro-acoustic analysis of an Efacec “15 MVA 25.6 / 2.6 kV YNd11” three-phase core type power transformer (see Figure 1), based on a FEM/BEM model. The development steps of simulation model, from the estimation of characteristic electromagnetic loading, up to the prediction of radiated power level, are briefly described in the next sections.

Figure 1: Efacec 15 MVA 25.6 / 2.6 kV YNd11 three-phase core type power transformer

3.3.1. Prediction of representative electromagnetic loading

Representative modeling of the electromagnetic loading is essential for vibro-acoustic studies, having a direct impact on the simulation accuracy. Therefore, although the discussion of results is focused on the vibro-acustic response of the power transformer, the assumptions related with the electromagnetic analysis are listed below.

Magnetostriction of electrical steel: The magnetostriction behavior induced by the magnetic field in the transformer core was included based on experimental data [13] (see Figure 2).

Magnetic behavior of electrical steel: Data of electrical steel manufacturers were considered to describe the magnetic properties of the transformer core. Grain oriented electrical steel is represented by anysotropic properties with diferent (in-plane) permeabilities in rolling and cross rolling directions [14, 15], as plotted in Figure 3.

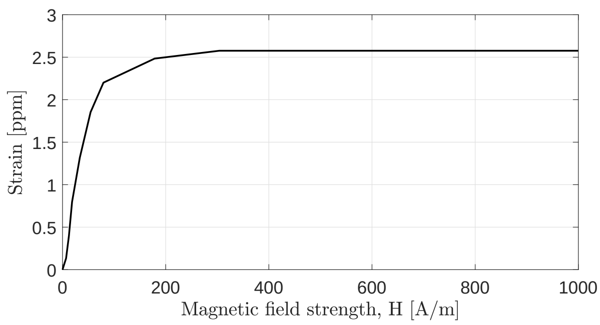

Figure 2: Typical magnetostriction in rolling direction

Besides, to take into account the effect of core lamination in the magnetic flux, an equivalent permeability in the out-of-plane direction was given, according to the stacking factor and magnetic reluctance definition.

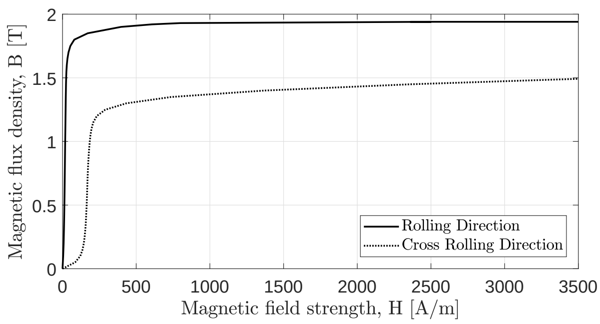

Figure 3: Typical B-H curves of electrical steel in rolling and cross-rolling directions

Equivalent air-gaps of the magnetic circuit: Reluctance forces occurs when the magnetic field faces a material with different magnetic permeability, such as in the air-gaps of the core joints. Aiming higher computational eficiency, the modelling of the joints between yokes and limbs with detailed step-laps, was replaced by an equivalent air gap (at 45° angle) passing through the entire cross section **[citação a justificar boa aproximação para altas induções]**, as depicted by Figure 4.

Load and No-Load operating conditions: At no-load condition, transformer's core excitation was accomplished by three windings, one for each core limb, with an AC supply voltage equal to the nominal voltage of primary winding side. The three phases are shifted as in a real three-phase power transformer.

In order to express the load condition, excitation was accomplish with nominal Amper-Turns supply in primary and secondary windings. Besides allowing to overcome the difficulty in characterizing the transformer load impedance, this approach also reproduces the procedure performed in the laboratory testing.

The reluctance and magnetostriction forces in the magnetic core, and the Lorentz forces in the windings, are predicted simulating the power transformer under the previously referred no-load and load conditions.

Under actual conditions, a power transformer operating at nominal power undergoes simultaneously those three types of electromagnetic loads. Therefore, after sincronizing

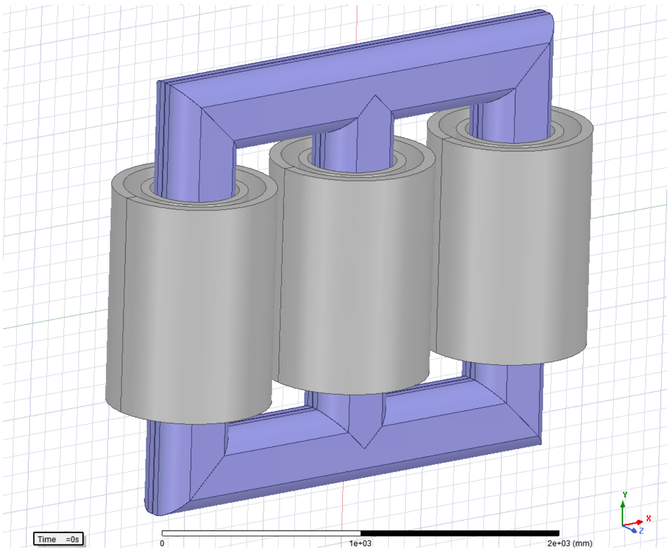

Figure 4: 3D Power Transformer Model Core and Coils Geometry

the phase of electromagnetic forces obtained from different electromagnetic simulations, they were all considered in the vibro-acustic simulation presented below.

3.3.2. Description of model implementation

As previously referred, the vibro-acoustic model addopted in this research to solve the interior/exterior problem is based on both FEM and BEM. In particular, BEM allowed to dicretize both the acoustic domains: insulation oil and surrounding air.

3.2.1 Structural domain

In order to extract the structural modal basis of the power transformer, a FEM model was developed, through commercial software, following state-of-the-art methodologies. The detailed CAD model (see Figure 1) was simplified as shown in Figure 5. This model considered typical properties for the materials of power transformers, such as: structural steel, copper alloy, pressboard, as well as material for electrical and vibration insulation. Additionally, as shown in Figure 5, radiators and bushings were simplified as discrete masses connected to the tank fixing regions; mass of oil pumps were neglected and replaced by a rigid connection between the respective piping terminals.

Considering the power transformer simply supported in its wheelset, two structural modal bases were extracted up to 500 Hz:

- **Modal Base #1:** corresponding to the real configuration of the power transformer;
- **Modal Base #2:** corresponding to a configuration in which the active part is radiating inside the transformer tank, without the structural paths. The supporting blocks in the bottom and upper part of the active part are considered as pinned, instead of being assumed as perfectly connected to the tank bottom and cover, respectively.

As shown in Figure 6, the boundary conditions applied to the active part in the Modal Base #2 allow to extract natural frequencies of vibration whose values evolve similarly to those of the Modal Base #1.

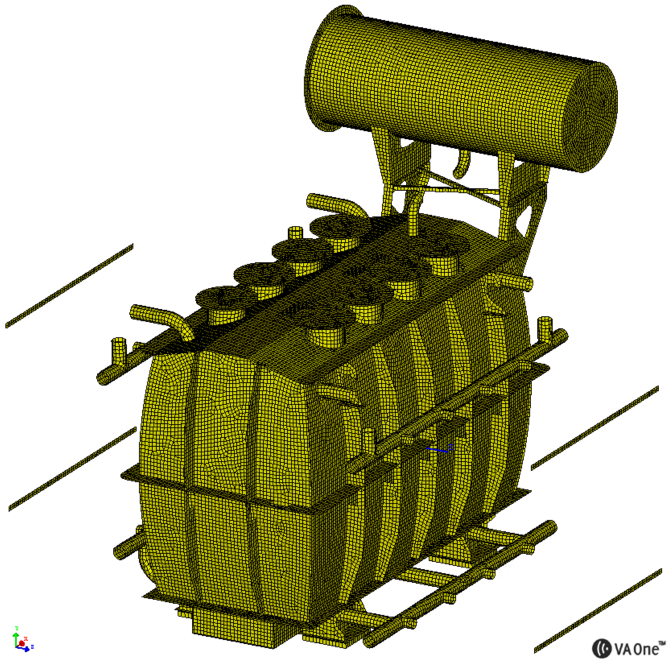

Figure 5: Meshed geometry of the structural FEM model

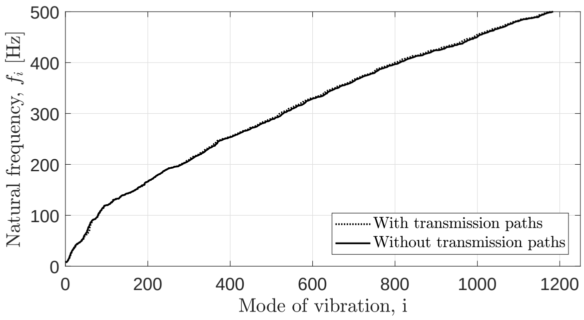

Figure 6: Natural frequencies of vibration included in the modal bases #1 and #2, extracted up to 500 Hz, respectively with and without structural transmission paths

3.2.2 Acoustic domains

Two acoustic domains were conidered: the inner insulation oil and the surrounding air. Characteristic sound speed, density and damping loss factor were adopted. Outter surfaces of the yokes and phases were considered as the major radiating surfaces.

In order to compare the results obtained for the different simulated scenarios, 18 equally spaced measurement sensors were defined around the transformer (see Figure 7), at half the height, and at approximatelly 300 mm from the tank surface or cooling devices, as would be recommended for experimental noise measurement [13].

3.3.3. Description of the case studies and analysis of results

Aiming to study the influence of acustic and stuctural transmission paths on the radiated noise level, and in order to quantify that influence, four analysis of the presented power transformer were considered:

- **Configuration A):** real scenario, with structural paths connecting the active part to

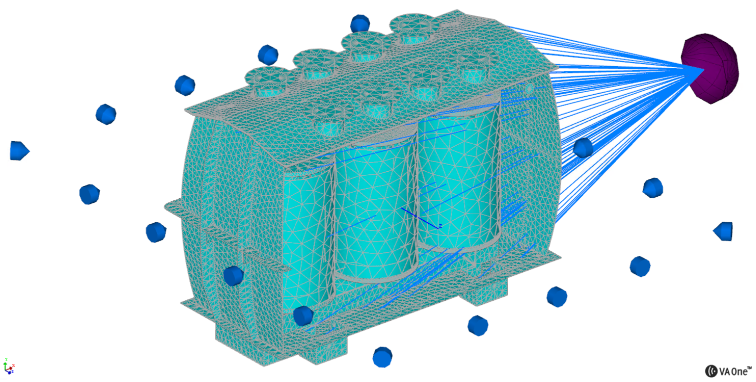

Figure 7: Acoustic model with hidden front pannel, showing: the surrounding point sensors and one of the BEM fluids (oil) connected to the inner tank and to the active part radiating surfaces

the oil-filled tank;

- **Configuration B):** with structural paths connecting the active part to the air-filled tank;
- **Configuration C):** without structural paths connecting the active part to the oil-filled tank;
- **Configuration D):** without structural paths connecting the active part to the air-filled tank.

For Configurations A and B (with structural paths), and for configurations C and D (without structural paths), the Modal Bases #1) and #2) were chosen, respectively. The spatially averaged sound pressure obtained for each configuration were calculated, and some relative values are available in Table 1.

Table 1: Ratio of sound pressures p_i/p_j, obtained for some pairs $\{i, j\}$ of configurations.

Configuration j	Configuration i A)	B)	C)	D)
A)	1	-		-
B)	1.38	1	-	-
C)	7113	-	1	-
D)	-	4.3×10^8	8.2×10^4	1

The analysis of obtained results, and in particular the ratio $p_{C)}/p_{D)} = 8.2 \times 10^4$, regarding configurations without structural paths, demonstrate that indeed the oil creates a very effective transmisson path, when compared with air. Besides, the ratio $p_{B)}/p_{D)} = 4.3 \times 10^8$, regarding configurations with an air-filled tank, also reveals, that as expected structural paths created by joining elements are extremely efficient in the transmission of noise and vibration.

Additionally, comparing the configurations with transmission paths ($p_{A)}/p_{B)}$), once again the oil creates a more efficient acoustic path than air; the predicted acoustic pressure values was increased in 38%.

The observed change caused by the oil when comparing configuration A) and B) - both with structural paths - is not so noticible than when comparing the configurations C) and D) - both without structural paths. These results can be partially justified by the fact that an alternative structural path, based on a direct coupling, is more efficient in this range of frequencies, than an acoustic path based on fluid-structure interaction.

However, the previous argument do not explain why in the presence of a structural path, the oil effect is able to increase the acoustic pressure of configuration B) in 38%, and at the same time, in the absence of that structural path - in configuration C) - the transmitted noise through the acoustic domain is negligible ($p_{A)}/p_{C)} = 7113$). These type of changes can also be explained by the frequency shift caused not only by an heavy fluid, but also by minor structural changes, which are able to modify the frequency response function, and in particular its local minimums/maximums. Such changes can have a significant impact in the radiated noise, as demonstrated by the discussed results.

4. CONCLUSIONS

A numerical study for the characterization of the transmission paths, aiming to evaluate their influence on the transformers noise is presented in this study. The numerical approach considered the multiphysics phenomena related to electromagnetic forces, structural vibrations and acoustics radiation in the fluid domain.

Noise transmission paths in a power transformer were divided in two major groups, the insulation oil (fluid-structure coupling) path and the structural path. The analysis of the oil transmission path is addressed in this study using the Boundary Element Method and the structural analysis using the Finite Element Method.

A core type power transformer was adressed in the case study. Obtained results show that, with structural paths, the acoustic transmission introduced by the insulation oil increased in 38% the radiated acoustic pressure. If the structural paths are neutralised, the numerical model shows an insignificant contribution of the oil. This result is justified by the fact that small changes in the frequency response of the power transformer can significantly affect the radiated noise level.

Indeed, through accurate simulation of the impact due to combined structural modifications and oil effect in the natural frequencies of vibration, the structural design can be optimized in order to match the local minimums of the frequency response with the main harmonics of the elecromagnetic loading.

5. ACKNOWLEDGEMENTS

This work is supported by the project POCI-01-0247-FEDER-024035, with the acronym *Quiet Transformer 2*, co-funded by the European Regional Development Fund (ERDF) through COMPETE2020 - Programa Operacional de Competitividade e Internacionalização (POCI) under the “Portugal 2020” Programme.

6. REFERENCES

[1] Lisa Goines, Louis Hagler, et al. Noise pollution: a modern plague. *Southern Medical Journal-Birmingham Alabama*, 100(3):287–294, 2007.

[2] Ravish S Masti, Wim Desmet, and Ward Heylen. On the influence of core laminations upon power transformer noise. In *Proceedings of ISMA*, pages 3851–3862, 2004.

[3] Vinod Rohilla and C. Palani. Samy. A study of transformer noise and reduction techniques of transformer noise. *Journal of Basic and Applied Engineering Research*, 2015.

[4] Liming Ying, Donghui Wang, Jinwei Wang, Guodong Wang, Xiaowen Wu, and Jiangtao Liu. Power transformer spatial acoustic radiation characteristics analysis under multiple operating conditions. *Energies*, 11(74), 2018.

[5] Moritz Kreutzer. Modelling of core noise from power transformers. Master's thesis, Royal Institute of Technology, School of Computer Science and Communication, 2011.

[6] Ming Jin and Jie Pan. Vibration transmission from internal structures to the tank of an oil-filled power transformer. *Applied Acoustics*, 113:1–6, 2016.

[7] Ming Jin, Jie Pan, Hai Huang, and Jianping Zhou. Transmission of vibration of a power transformer from the internal structures to the tank. In *Acoustics 2012*, Fremantle, Australia, 2012.

[8] M Rausch, M Kaltenbacher, H Landes, R Lerch, J Anger, J Gerth, and P Boss. Combination of finite and boundary element methods in investigation and prediction of load-controlled noise of power transformers. *Journal of Sound and Vibration*, 250(2):323–338, 2002.

[9] Noureddine Atalla and Franck Sgard. *Finite element and boundary methods in structural acoustics and vibration*. CRC Press, 2015.

[10] John David Jackson. *Classical electrodynamics*. Wiley, New York, 3rd edition, 1999.

[11] Satish V Kulkarni and S A Khaparde. *Transformer engineering: design, technology, and diagnostics*. CRC Press, 2013.

[12] Luis Rodriguez-Tembleque, José González, Antonio Cerrato, and Ramón Abascal. Non-symmetrical be-fe partitioned formulation for acoustic fluid-structure interaction problems. 06 2013.

[13] IEC 60076-10-1: 2016. Power transformers - part 10-1: Determination of sound levels - application guide, 2016.

[14] Powercore ® H. Technical report, Thyssenkrupp Electrical Steel GmbH.

[15] Cheng Zhiguang, Norio Takahashi, and Behzad Forghani. Team problem 21 family (v. 2009). *International Compumag Society Board at Compumag (2009).*